Kilogram scale throughput performance of the KATRIN tritium handling system

Michael Sturm *, Florian Priester, Marco Röllig, Carsten Röttele, Alexander Marsteller, David Hillesheimer, Lutz Bornschein, Beate Bornschein, Robin Größle, Stefan Welte

Karlsruhe Institute of Technology, Institute for Astroparticle Physics, Tritium Laboratory, Karlsruhe, Germany

ABSTRACT

The Karlsruhe Tritium Neutrino (KATRIN) experiment aims to determine the effective mass of the electron antineutrino by investigating the tritium β-spectrum close to the energetic endpoint. To achieve this, there are stringent and challenging requirements on the stability of the gaseous tritium source. The tritium loop system has the task to provide the <0.1 % stabilized flow rate of tritium gas into the KATRIN source with a throughput of 40 g/day and a tritium purity>95 %. KATRIN started full tritium operation in early 2019. This paper focusses on the observed radiochemical effects and confirms that non-negligible quantities during initial tritium operation have to be expected.

1. Introduction

The KATRIN experiment aims at the determination of the effective mass of the electron antineutrino with a projected sensitivity of 0.2 eV/c^2 (90 % confidence level) [1]. After first campaigns with deuterium and traces of tritium [2,3], KATRIN started full tritium operation in early 2019. With the first full tritium measurement campaign, a new upper limit of 1.1 eV/c^2 for the neutrino mass was found [4].

After a brief description of the tritium handling (*Loop*) system followed by a recap of the performance of the first 150 d of full T_2 operation, the focus is set to the observed radiochemical reactions at the inner surfaces of the *Loop* system.

2. The KATRIN tritium *Loop* system

The tritium *Loop* system and its requirements are described in detail in [5] and [6], with the operational requirement of 24/7 operation at a throughput of 40 g/d.

Fig. 1 shows a simplified flow diagram of the *Loop* system. Tritium is injected from a pressure controlled buffer vessel over a transfer line and capillary into the injection chamber in the middle of the WGTS beamtube (**w**indowless **g**aseous **t**ritium **s**ource). The capillary, injection chamber and beamtube are operated at ≈30 K (stabilized to 0.1 %) [7]. The gas is pumped out by a cascaded pumping system (DPS1) consisting of 14 TMPs [8] (**t**urbo**m**olecular **p**ump) type Leybold MAG W2800

located at pumpports at both ends of the WGTS (**w**indowless **g**aseous **t**ritium **s**ource) beamtube. Four groups of MAG W2800 are each pumped by a Pfeiffer HiPace300 pump. The forevacuum is provided by a Normetex/Metal bellows combination which pushes the gas through a palladium membrane filter ("permeator") in a buffer vessel. From there the gas is led over a Laser Raman sampling cell [9] and a regulation valve back into the pressure-controlled buffer vessel. At the permeator non-hydrogen components are removed from the gas stream. In order to avoid blocking of the permeator due to impurity accumulation over time, a certain amount of gas ("bleed") is continuously extracted on the high-pressure side of the permeator and collected in the *Exhaust Loop*. The amount of gas not recirculated is continuously replaced from the *Feed Loop* which is supplied batch wise with gas from TLK infrastructure.

At the rear end of the WGTS the CMS (**c**alibration and **m**onitoring **s**ystem) [10] is attached, containing two TMPs. Downstream, the DPS2 (**d**ifferential **p**umping **s**ection) [11], consisting of four pumpports and six TMPs, and the CPS (**c**ryogenic **p**umping **s**ection) [12] are attached. The combination of DPS and CPS reduces the gas flow rate towards the spectrometers by >14 orders of magnitude. Gas pumped off at CMS and DPS2 is collected in the *Exhaust Loop* and not recirculated.

The overall *Loop* system consists of 33 TMPs, 4 Normetex/Metal Bellows combinations, ≈220 sensors and ≈230 valves. Tritium operation involves the whole TLK infrastructure, the interfaces (**t**ritium **t**ransfer **s**ystem TTS, **i**sotope **s**eparation **s**ystem ISS and CAPER) and combined operation are described in [13,14].

---

* Corresponding author.
  E-mail address: michael.sturm@kit.edu (M. Sturm).

3. Tritium commissioning of the system

After commissioning the system with deuterium and a ≈1% tritium in deuterium mixture (in chemical state as DT in D_2) in 2018, operation with tritium of >95 % purity started in 2019. This section describes the performance of the system with T_2 and the observed effects.

3.1. Initial high throughput tritium operation

Full tritium operation started in the first quarter of 2019. The throughput over the WGTS beam tube was ramped up stepwise by increasing the pressurecontrolled buffer vessel pressure (Fig. 2). Whereas in the first days stable operation was achieved, the throughput started to rapidly decrease after a few days of operation, first visible at the 32.5 sccm (standard cm^3 per minute) setting.

This decrease can be explained by the geometry of the injection capillary. The injection line inside the WGTS cryostat is fixed to LN_2 temperature at the point where the inner pipe diameter is reduced from 6 mm to 2.1 mm. After further 0.9 m, the remaining 4.9 m of the injection capillary are thermally coupled to the beamtube (≈30 K). In principle any gas species apart from hydrogen isotopologues, neon and helium could freeze out inside the injection capillary at 30 K and form an orifice which – once the aperture diameter is reduced to such extent that it dominates the overall conductance – decreases the throughput at a given buffer vessel setpoint significantly.

Such a decrease was not observed during the deuterium only and low tritium content commissioning in 2018 [2]. All impurities originating from the TMPs and beamtube are removed by a permeator and the gas batches from TLK infrastructure are transferred to the *Loop* system over a second permeator. This excludes external contributions leaving an internal production of impurities induced by radiochemical reaction in between the permeators and the injection capillary. A known impurity generated by radiochemical reactions in tritium containing systems in combination with stainless steel surfaces is tritiated methane [15,16]. This formation of tritiated methane and possibly other impurities by radiochemistry strongly depends on the amount of carbon available at the inner surfaces. This amount can be much higher than in the bulk [17]
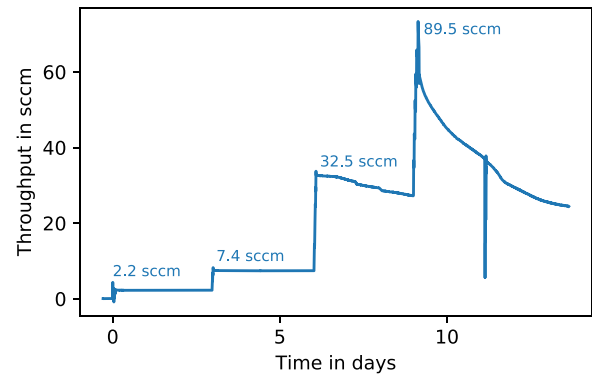
Fig. 2. Decrease of throughput during the first 14 days of operation. The throughput was increased by raising the setpoint of the injection buffer pressure stepwise. The corresponding flow rates, which would have been reached without the decrease in conductance due to freeze-out of impurities, are given in the picture.

but decreases over time as carbon is used up in radiochemical reactions.

3.2. Identification of tritiated methane and CO

After 14 days the injection was stopped, capillary as well as beamtube were warmed up to ≈80 K. Fig. 3 shows the pressure reading of a capacitive-type pressure sensor attached to the injection chamber during the warm-up. Two peaks of gas release were detected and identified by a simultaneous mass spectrometer measurement as mass 28/CO and tritiated methane species (mainly mass 24/CT_4). Release only occurred after the beamtube had reached ≈80 K. Therefore it can be concluded that the observed tritiated methane and CO were frozen in between the LN_2 coupled part of the injection capillary and the 30 K part.

3.3. Consecutive high T_2 throughput operation

After the 1st warm up the WGTS was cooled down again to ≈30 K
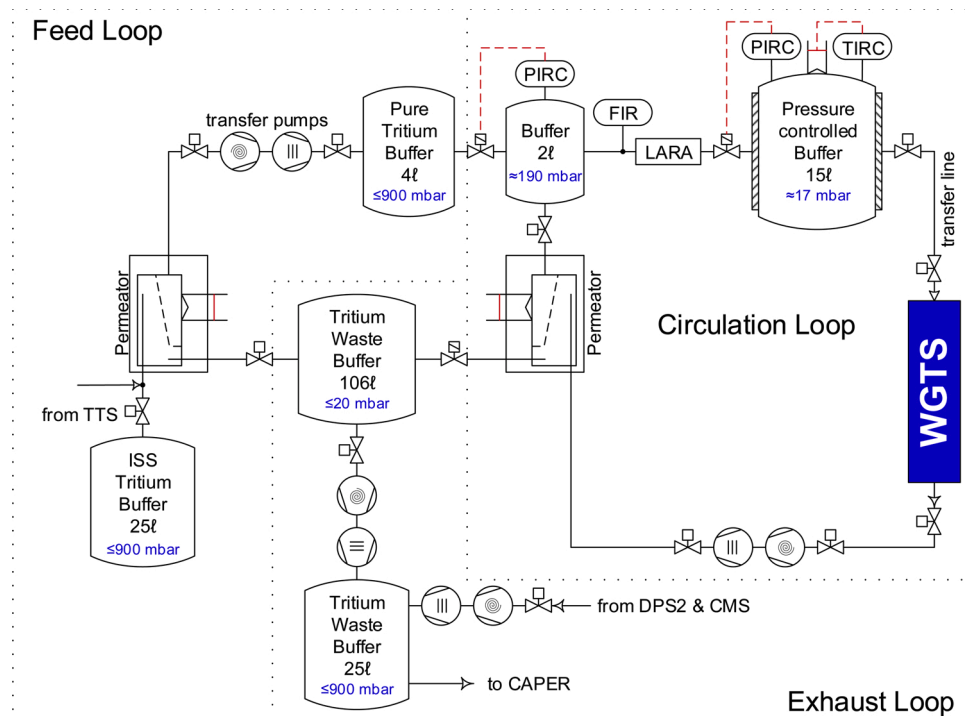
Fig. 1. Simplified flow scheme of the KATRIN tritium loop system. The pumping systems at WGTS consists in total of 18 TMPs. DPS2, CMS and CPS are not shown.
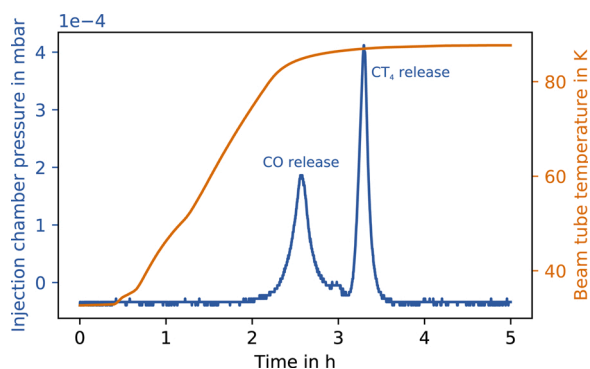
Fig. 3. Release of CO and tritiated methane during first warm-up.

and circulation was resumed at 13.5 sccm flow rate. A throughput value on the level of the first ramp up was reached, verifying that only CO and tritiated methane contributed to the partial blocking of the injection capillary and no or negligible amounts of other species were frozen inside the capillary.

A 2nd warm up to 80 K level was performed after further 35 days of operation when the throughput again slowly started to decrease.

A 3rd warm up to 80 K level was performed after further 19 days of operation. Prior to warming up 2 days of operation at 89.5 sccm gas flow rate were performed, resulting in a stability of 0.13 %/day. This already is a factor >100 better compared to the initial stability at this set point.

The bleed value at the *Circulation Loop* permeator was set to a constant value of 1.4 sccm. The tritium purity of the circulated gas during the 1st tritium measurement campaign was >97 % [18].

4. Approximation of methane and CO generation

4.1. Quantification of released methane and CO

The amount of gas released during a warm-up of the WTGS beamtube was estimated by collecting the released gas of the warm-up in a closed volume behind the roughing pumps.

During 1st warm-up, a release of 8 ± 2 cm^3 (STP) of gas was observed, during 2nd warm-up 3 ± 0.5 cm^3 and third warm-up 0.8 ± 0.2 cm^3. The amount decreases with prolonged tritium exposure pointing to a significantly reduced impurity gas generation during standard operation.

The sum of the released gas amount during the three warm-ups however is not identical to the amount of CO and methane generated in total: After the 1st warm-up the beam tube stayed at $\approx$80 K for 7 days, after the 2nd warm-up for 2 days only. During that time, the *Loop* system stayed exposed to tritium and was evacuated before resuming circulation. Impurities generated in these time periods were not accounted for. Taking into account the decreasing generation rate, an upper limit for the total amount of impurities being generated in the first 78 days of 16 cm^3 can be assumed.

4.2. Review of literature data

Methane generation is strongly dependent on the surface quality: Morris [15] and Gill [16] investigated tritium induced methane production of various stainless steel surface qualities at room temperature and 100 °C. All samples showed the highest production rate directly after start of tritium exposure. The rate declines with exposure time. For samples with non-degreased surfaces or samples with special coatings, increased methane generation rates were reported, compared to all other investigated samples. The rates were higher than one order of magnitude. Maximum generation rates were observed for the "as received and rinsed" sample in [15] and the "chemical conversion aluminum" sample in [16].

An additional information can be gained from these publications by comparing the impurity generation rates to the ^{3}He generation rate: the maximum generation rate of methane stayed below the level of the ^{3}He generation rate corresponding to the stated tritium amounts and exposure time for almost all the samples. This indicates that in average less than one molecule of methane per decay inside the volume was created due to radiochemical reactions at the inner surface. The only data deviating are the initial days shown for the non-degreased "as received and rinsed samples" in [15]. For these dedicated samples no measurements with deuterium were reported which could have determined to which extent outgassing of carbon containing species from the non-degreased surfaces could have contributed to the observed methane build-up.

A similar observation is shown in the publication of Coffin [19] investigating methane generation from tritium-graphite interaction and tritium stainless steel interaction: the amount of methane reported there was below the amount of ^{3}He being generated in the reported time. Neither of the mentioned publications reported or investigated creation of CO. Possible mechanism leading to tritiated methane and CO are electron [20] and ion [21] stimulated desorption of CH$_4$ and CO, radiolysis of impurity surface films [22], and subsequent isotope exchange reactions inside the gas phase [23]. Other candidates are directly triggered reactions by T$^+$ and T^{3+} ions. Most likely one observes a superposition of various effects.

4.3. Inner surfaces of Loop system

The inner surface of the *Loop* system consists of anodically cleaned surfaces of the piping and the metallic blank surfaces of the loop buffer vessels. The system underwent a final cleaning and degreasing procedure prior to installation. Table 1 gives an overview of the volumes and surface areas of the relevant parts of the *Loop* system. Also given are the mean pressure and corresponding activities during the initial 14 and 78 days of operation. As a reference, the calculated integral amount of ^{3}He created by tritium decay during that time is given.

Morris and Gill reported a generation of tritiated methane of up to 20 cm^3/m^2 for comparable surfaces. Within the initial 14 days of KATRIN tritium operation $\approx$8 cm^3 of impurities were generated, the upper limit for impurity generation after 78 days was 16 cm^3. This value is in agreement with the reported value.

4.4. Carbon exhaustion by tritium exposure

The amount of methane and CO produced during the initial 14 days is less than the amount of ^{3}He being generated in the same time. It is hereby assumed that per one decay in a given volume max. One radiochemical reaction at the surface can take place. From the numbers given in the table it is concluded, that carbon depletion of the pressure-controlled buffer vessel and transfer line surfaces – the parts with the largest surfaces, but also the lowest operation pressures – was not reached after the initial 78 days of tritium exposure. The total amount of ^{3}He being created in these volumes is far less than the expected amount of impurity generation from the surfaces. Therefore, the relevant part of the system was statically exposed to $\approx$680 mbar of tritium for 5 weeks in order to use up the remaining carbon at the surfaces.

4.5. Performance after tritium exposure

The 2nd tritium measurement campaign of KATRIN was performed during the 2nd half of 2019 with an injection flow of $\approx$90 sccm. There was no evidence for a freeze-out of methane or CO over a period >60 days. This verifies the success of the described counter measure to reduce the methane generation.

Table 1
Surface areas, volumes and tritium amounts inside the system during first tritium operation.

	Transfer pumps	4ℓ vessel	2ℓ vessel	15ℓ vessel	Transfer line	$\sum$
Volume (ℓ)	0.75	4	2	15	5.2	27
Surface (m^2)	0.3	0.16	0.1	0.32	0.84	1.7
			Initial 14 days			
Mean pressure (mbar)	252	615	190	9	9	
Mean amount (mbarℓ)	189	2460	379	136	47	3211
Mean activity (Bq)	1.8E+13	2.3E+14	3.6E+13	1.3E+13	4.4E+12	3.0E+14
^{3}He/d (cm^3/d)	5.8E-02	7.6E-01	1.2E-01	4.2E-02	1.4E-02	9.9E-01
^{3}He integral (cm^3)	0.8	10.6	1.6	0.6	0.2	13.9
			Initial 78 days			
Mean pressure (mbar)	236	597	188	8	8	
Mean amount (mbarℓ)	177	2388	376	121	42	3103
Mean activity (Bq)	1.7E+13	2.3E+14	3.6E+13	1.1E+13	4.0E+12	2.9E+14
^{3}He/d (cm^3/d)	5.4E-02	7.3E-01	1.2E-01	3.7E-02	1.3E-02	9.5E-01
^{3}He integral (cm^3)	4.2	57.3	9.0	2.9	1.0	74.4

5. Conclusion

The KATRIN tritium handling system was successfully operated for more than 150 days with tritium within the first two measurement phases and has proven its capability to be operated continuously for >60 days. In the beginning of tritium operation, radiochemical reactions were observed, leading to the creation of tritiated methane and CO. This ultimately caused a decrease in overall throughput due to freezing out and blocking inside the injection capillary. By exposition of the inner surfaces to tritium they were successfully depleted of carbon. Potential remaining generation of impurities in radiochemical reactions at the inner surfaces is now reduced to a level not influencing the throughput performance any more.

As a comparative number for the generation rate of radiochemical products, the ^{3}He generation rate was identified which in turn can also be used for approximating exposure times and pressures needed for a given geometry in order to deplete it from carbon.

Furthermore, enrichment of non-hydrogen impurities in the closed *Loop* gas stream has been successfully suppressed by the use of the permeators. The tritium purity could be held > 97 % during the whole tritium campaign.

After carbon exhaustion by tritium exposure the *Loop* system has proven its capability to run 24/7 for >60 days with tritium at a throughput of ≈40 g/d while matching the specifications for tritium purity and source stability. This was achieved while only 1.4 sccm (≈1%) of gas was lost to the *Outer Loop* - mainly the required extraction of gas in front of the permeator - needing to be continuously replaced. In 2019 a total tritium throughput of ≈3 kg has been reached.

Declaration of Competing Interest

The authors report no declarations of interest.

Acknowledgments

References

[1] J. Angrik, et al., (KATRIN Collaboration), KATRIN Design Report, Wissenschaftliche Berichte, FZ Karlsruhe 7090, 2004, https://doi.org/10.5445/IR/270060419.

[2] M. Aker, et al., First operation of the KATRIN experiment with tritium, Eur. Phys. J. C 80 (2020) 264, https://doi.org/10.1140/epjc/s10052-020-7718-z.

[3] F. Priester, et al., Tritium processing systems and first tritium operation of the KATRIN experiment, Fusion Sci. Technol. 76 (4) (2020) 600–604, https://doi.org/10.1080/15361055.2020.1730118.

[4] M. Aker, et al., Improved upper limit on the neutrino mass from a direct kinematic method by KATRIN, Phys. Rev. Lett. 123 (2019), 221802, https://doi.org/10.1103/PhysRevLett.123.221802.

[5] O. Kazachenko, et al., Tritium processing loop for KATRIN experiment, Fusion Sci. Technol. 54 (1) (2008) 67–70, https://doi.org/10.13182/FST08-A1766.

[6] F. Priester, et al., Commissioning and detailed results of KATRIN inner loop tritium processing system at Tritium Laboratory Karlsruhe, Vacuum 116 (2015) 42–47, https://doi.org/10.1016/j.vacuum.2015.02.030.

[7] F. Heizmann, et al., The windowless gaseous tritium source (WGTS) of the KATRIN experiment, J. Phys. Conf. Ser. 888 (2017) 012071, https://doi.org/10.1088/1742-6596/888/1/012071.

[8] F. Priester, et al., TriTop – a compatibility experiment with turbomolecular pumps under tritiumatmosphere, Vacuum Volume 98 (December) (2013) 22–28, https://doi.org/10.1016/j.vacuum.2012.09.006.

[9] S. Fischer, et al., Monitoring of tritium purity during long-term circulation in the KATRIN test experiment LOOPINO using Laser Raman Spectroscopy, Fusion Sci. Technol. 60 (3) (2011) 925–930, https://doi.org/10.13182/FST11-A12567.

[10] M. Babutzka, et al., Monitoring of the operating parameters of the KATRIN windowless gaseous tritium source, New J. Phys. 14 (2012) 103046, https://doi.org/10.1088/1367-2630/14/10/103046, 29pp.

[11] A. Marsteller, et al., Neutral tritium gas reduction in the KATRIN differential pumping sections, Vacuum Volume 184 (February) (2021) 109979, doi:j.vacuum.2020.109979.

[12] W. Gil, et al., The cryogenic pumping section of the KATRIN experiment, Ieee Trans. Appl. Supercond. 20 (June (3)) (2010) 316–319, https://doi.org/10.1109/TASC.2009.2038581.

[13] S. Welte, et al., Experimental performance test of key components of the KATRIN outer tritium loop, Fusion Sci. Technol. 71 (3) (2017) 316–320, https://doi.org/10.1080/15361055.2017.1291233.

[14] S. Welte, et al., Tritium supply and processing for the first KATRIN tritium operation, Fusion Sci. Technol. 76 (3) (2020) 227–231, https://doi.org/10.1080/15361055.2019.1705681.

[15] G.A. Morris, Methane formation in tritium gas exposed to stainless steel. Lawrence Livermore Laboratory Report, UCRL-52262, 1977, https://doi.org/10.2172/7320371.

[16] J.T. Gill, Effect of container preparation on the growth of protium and methane impurities into tritium gas, J. Vac. Sci. Technol. 17 (1980) 645, https://doi.org/10.1116/1.570532.

[17] J.T. Gill, et al., Chemically polished stainless steel tubing for tritium service, J. Vac. Sci. Technol. A 1 (1983) 869, https://doi.org/10.1116/1.572012.

[18] M. Aker, et al., Quantitative long-term monitoring of the circulating gases in the KATRIN experiment using Raman spectroscopy, Sensors 20 (2020) 4827, https://doi.org/10.3390/s20174827.

[19] D.O. Coffin, C.R. Walthers, Methane Generated from Graphite-tritium Interaction, Los Alamos Scientific Laboratory Report LA-7627-MS, 1979, https://doi.org/10.2172/6280302.

[20] O. Malyshev, Electron stimulated desorption from the 316 L stainless steel as a function of impact electron energy, J. Vac. Sci. Technol. A31 (2013) 031601, https://doi.org/10.1116/1.4798256.

[21] A.G. Mathewson, Ion Induced Desorption Coefficients for Titanium Alloy, Pure Aluminum and Stainless Steel, CERN ISR VA/76-5, 1976. https://cds.cern.ch/record/314510.

[22] G. Földiák, Radiolysis of liquid hydrocarbons, Radiat. Phys. Chem. (1977) 16 (6) (1980) 451–463, https://doi.org/10.1016/0146-5724(80)90191-0.

[23] T.H. Pratt, et al., The self-induced exchange of tritium gas with methane, J. Am. Chem. Soc. 83 (1) (1961) 10–17, https://doi.org/10.1021/ja01462a002.